Proceedings of the 17th International Conference on Force, Mass, Torque and Pressure Measurements,
IMEKO TC3, 17-21 Sept. 2001, Istanbul, Turkey

Error Analysis for Gyroscopic Force Measuring System

Shigeru Kurosu*, Kazuhiro Kodama**,Motoyuki Adachi***, Kazuyuki Kamimura****

*Oyama National Collage of Technology, Oyama, Japan
**Kyushu Institute of Technology, Iizuka, Japan
***Yamamoto Scale Co., Ltd., Akashi, Japan
****Yamatake Building Systems Co., Ltd, Tokyo, Japan

Abstract

This paper concerns the development of a new type of force sensor called Gyroscopic Force Measuring System, (simply called GFMS) for measuring a force vectorialy. The GFMS realized a highly accurate measurement using an estimator for the unknown angles of incidence of a force vector. The estimator, however, assumed an exact knowledge on the dynamical equations in the steady-state. This caused much degradation in the measurement accuracy unless the steady-state of the GFMS could be attained. The estimation errors of the angles of incidence directly affect the accurate measuring of the force. We can get the better performance by choosing the adequate damping coefficient of gyroscope (for nutation mode). From the error analysis, some essential information for designing the GFMS is highlighted.

1. Introduction

The early part of the twenties century saw gyroscopes being applied to a variety of fields. It has been used to navigate ships and rockets, to stabilize the rolling of ships, to counter vibration and to operate innumerable control mechanisms. The small directional unit of the gyro-compass operates by the same principles as the massive rotor of the ship stabilizer. Today, this mechanical gyros consist of a rotor spinning rapidly about its axis would be difficult to find in industrial application fields. This is because special devices for the sensor using entirely different principles have been emerged. For example, fiber-optic gyros, quartz vibrating gyros and the like have been con- ceived in stead of traditional mechanical gyros.

In this paper, of particular interest to us is how to apply the unique features of mechanical gyros for a force sensor. Three decade ago, a new type of mechanical gyro for measuring a force was invented and produced in Germany. The original Gyroscopic Force Measuring System, (simply called GFMS) has earned much interest as a weighing scale due to its advantages of high resolution [1]～[3]. This principle can easily be extended to the measurement of a vectorial force in space.

This paper explores the possibility of the GFMS to the vectorial measurement of a force. An analysis in this study allows us to design the GFMS with suitable parameters to offer a reasonable accuracy. The total performance of the GFMS is demonstrated by numerical simulations. Some systematic errors associated with the GFMS are analyzed and discussed.

2. Basic Principle and Equations of Motion

2.1 Construction and Principle

Figure. 1 shows a construction model of the GFMS schematically. The vertical gimbal G_1, which supports the rotor, is free to rotate relative to the horizontal gimbal G_2 about *OX*, while the G_2 is free to rotate relative to the inner turntable G_3 about *OY*. The G_2 supports one end of a pivoted lever vertically. The other end of this lever is mounted on the G_1 at one end of the spin-axis of the rotor. The inner and outer turntables G_3 and G_4, which support the gyroscope, are free to rotate relative to the G_4 about *OZ* and the frame about *OX*, respectively. The force to be measured acts vectorially on the center of the lever through a swivel and therefore applies a force on one end

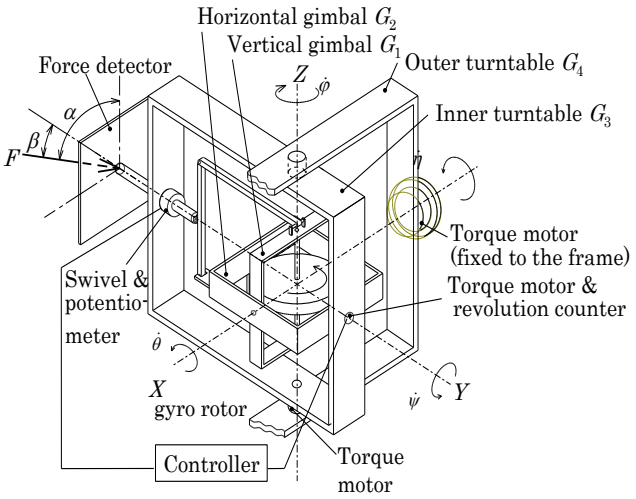

Figure 1. Construction model of GFMS

of the spin-axis of the rotor at the unknown angles of incidence α and β. The best estimated angles α and β can easily be defined as estimates for which the force *F* will be at the maximum value. The servomechanisms of the G_3 and G_4 serve this purpose even better because the algorithm can be easily programmed. This principle of the GFMS is somewhat similar to that of a well-known weathercock. The reason for this is that to

control the force detector's aspect perpendicular to the direction of the force in space is of dominant importance. The torque generated by the force applied causes the rotor in its gimbals to turn (called precession) about *OY* and the precession rate $\omega = \dot{\psi}$ is directly proportional to the force *F* applied.

When the rate ω can be measured accurately, the GFMS operates as a precise linear force transducer as follows:

$$\omega = -\frac{a}{H_0}F \tag{1}$$

where *F* is the magnitude of the force, H_0 is the spin angular momentum of the gyro-rotor and $2a$ is the length of a lever arm.

2.2. Analytical Description

To consider now the operation of the GFMS as shown in Figure 1 with the vertical spin-axis *OZ* and to point the output axis *OY* toward the direction of the force *F*, we assume that the force vector *F* which acts on the force detector can be defined by two rotations, namely α about *OX* and β about *OZ*. The equations of motion in this system can be described as follows:

$$\left.\begin{aligned}
&A\ddot{\theta} + c_1\dot{\theta} + H_0\dot{\psi} = T_{1x1}\\
&B\ddot{\psi} + c_2\dot{\psi} - H_0\dot{\theta} = T_{2y2}\\
&(C + D_1\cos^2\psi + D_2\cos^2\psi)\ddot{\varphi}\\
&\quad + \{c_3 + (D_2 - D_1)\dot{\psi}\sin\psi\cos\psi\}\dot{\varphi}\\
&\quad = T_{1x1}\sin\psi - T_{3z3}\\
&(E + F_1\cos^2\varphi + F_2\sin^2\varphi)\ddot{\eta}\\
&\quad + \{c_4 + (F_2 - F_1)\dot{\varphi}\sin\varphi\cos\varphi\}\dot{\eta}\\
&\quad = T_{1x1}\cos\varphi\cos\psi + T_{2y2}\sin\varphi - T_{4x4}
\end{aligned}\right\} \tag{2}$$

where *A*, *B*, *C* and *E* are the moments of inertia about *OX* and *OY* of gimbals and turntables, D_1 and D_2 are the moments of inertia including G_1 about *OZ* and G_2 about *OX*, F_1 and F_2 are the moments of inertia of the G_3 about *OX* and *OY*, T_{1x1}, T_{2y2}, T_{3z3} and T_{4x4} are the torques applied about *OX*, *OY*, *OZ* and *OX*, and c_1,c_2,c_3 and c_4 are the viscous friction coefficients about *OX*, *OY*, *OZ* and *OX*, respectively.

The feedback torques exerted on the G_2, G_3 and G_4 by the torque motors are given by

$$\left.\begin{aligned}
T_{2y2} &= k_p\theta + k_i\int_0^t \theta dt - k_d\dot{\psi}\\
T_{3z3} &= K_{P3}(\varphi - \varphi_r) + K_{D3}\dot{\varphi}\\
T_{4x4} &= K_{P4}(\eta - \eta_r) + K_{D4}\dot{\eta}
\end{aligned}\right\} \tag{3}$$

where k_p, k_i and k_d are the proportional, integral and derivative gains of the torque motor, K_{P3}, K_{I3} and K_{D3} are the proportional, integral and derivative gains of the torque motor, and η_r and φ_r are the reference inputs for the servo mechanisms. The controlled outputs η and φ are relative rotations of the turntables G_3 and G_4.

The external torque T_{1x1} supplied by the force F to the gimbal G_1 can be written as

$$\begin{aligned} T_{1x1} = & -Fa\{\cos\beta\cos\varphi\cos(\alpha+\eta) \\ & -\sin\beta\sin\varphi+\theta\cos\psi\cos\beta\sin(\alpha+\eta) \\ & -\theta\sin\psi\{\cos\beta\sin\varphi\cos(\alpha+\eta) \\ & +\sin\beta\cos\varphi\}\,. \end{aligned} \tag{4}$$

2.3. Estimations of α and β

The steady-state value of the output $\dot{\psi}=\omega$ can be written as

$$\omega = -\frac{Fa}{H_0}\{\cos\beta\cos\varphi_r\cos(\alpha+\eta_r) - \sin\beta\sin\varphi_r\}\quad . \tag{5}$$

If any three sets of reference inputs are excited as (η_{r0},φ_{r0}), (η_{r1},φ_{r1}) and (η_{r2},φ_{r2}) sequentially, the outputs ω_0, ω_1 and ω_2 for each of them can be obtained. The best estimates $\hat{\alpha}$ and $\hat{\beta}$ can be obtained by

$$\tan\hat{\alpha} = \frac{A_0B_1 - A_1B_0}{A_2B_0 - A_0B_2} \tag{6}$$

where

$$\left.\begin{aligned} A_0 &= \omega_0\sin\varphi_{r1} - \omega_1\sin\varphi_{r0} \\ A_1 &= \omega_0\cos\varphi_{r1}\cos\eta_{r1} - \omega_1\cos\varphi_{r0}\cos\eta_{r0} \\ A_2 &= \omega_1\cos\varphi_{r0}\sin\eta_{r0} - \omega_0\cos\varphi_{r1}\sin\eta_{r1} \\ B_0 &= \omega_1\sin\varphi_{r2} - \omega_2\sin\varphi_{r1} \\ B_1 &= \omega_1\cos\varphi_{r2}\cos\eta_{r2} - \omega_2\cos\varphi_{r1}\cos\eta_{r1} \\ B_2 &= \omega_2\cos\varphi_{r1}\sin\eta_{r1} - \omega_1\cos\varphi_{r2}\sin\eta_{r2} \end{aligned}\right\} \tag{7}$$

When $\hat{\alpha}$ is estimated, then $\hat{\beta}$ can easily be obtained by

$$\tan\hat{\beta} = \frac{\omega_1\cos\varphi_{r0}\cos(\alpha+\eta_{r0}) - \omega_0\cos\varphi_{r1}\cos(\alpha+\eta_{r1})}{\omega_0\sin\varphi_{r1} - \omega_1\sin\varphi_{ro}}\,. \tag{8}$$

2.4. Characteristic Values of GFMS

We have constitutionally two oscillatory modes, called precession and nutation modes, respectively. Two natural frequencies and damping coefficients are given by

$$\left.\begin{aligned} p_1 &= \sqrt{\frac{k_i}{H_0}}\quad , \quad \zeta_1 = \frac{k_p}{2\sqrt{H_0k_i}} \\ p_2 &= \frac{H_0}{\sqrt{AB}}\quad , \quad \zeta_2 = \frac{k_d}{2H_0}\sqrt{\frac{A}{B}} \end{aligned}\right\} \tag{9}$$

For conventional gyroscopic sensors, it is usually permissible to neglect p_2 assuming that $p_{2>>}\ p_1$. In designing our GFMS, p_2 cannot be neglected because increasing H_0 will decrease the sensitivity, as expressed in Equation 1. So, there exists some limitations on H_0 to measure a small force. The natural frequencies and damping coefficients for servomechanisms are given by

$$\left.\begin{aligned} p_{s3} &= \sqrt{\frac{K_{P3}}{C}},\quad \zeta_{s3} = \frac{K_{D3}}{2\sqrt{CK_{P3}}} \\ p_{s4} &= \sqrt{\frac{K_{P4}}{E}},\quad \zeta_{s4} = \frac{K_{D4}}{2\sqrt{EK_{P4}}} \end{aligned}\right\} \tag{10}$$

To attain the gain attenuation of turntables to disturbance torques less than -40 [dB], we have

$$K_P \geq 100 \tag{11}$$

3. Design and Construction of GFMS

3.1. Design Specifications

The foregoing consideration allows us to

design the GFMS. The design specifications are determined as,

- Measurable force range 0~0.3 [N]
- Measurable output range 20~40[rad/s]
- Measuring error (within 10 [s]) $\leqq 10^{-6}$[N]
- Gain attenuation of turntables (to reaction torques) $\leqq$ -40 [dB]

The constants of the gyro are summarized in Table 1. The characteristics and the feedback loop gains of the GFMS and the turntables are given in Table 2 and 3.

Table1. Characteristics of gyro-rotor

mass of gyro-rotor M	2.24×10^{-2} kg
moment of inertia I_z	1.45×10^{-6} kgm^2
revolution n	24000 rpm
spin angular moment H_0	0.37×10^{-2} kgm^2/s
length of lever system $2a$	5.5×10^{-2} m

Table2. Characteristics of gyro-sensor

natural frequencies	p_1	5.0 rad/s
	p_2	421.8 rad/s
damping coefficients	ζ_1	1.0
	ζ_2	0.1
feedback loop gains	k_p	3.70×10^{-2}
	k_i	9.25×10^{-2}
	k_d	2.68×10^{-3}

3.2. Construction of GFMS

An example of prototype GFMS is shown in Figure 2. Frictional torques in two swivels will cause instrumental errors. In the figure, to transmit the force acting on the detector to the gyro-rotor without loss of accuracy, flexure pivots and steel belts are arranged in place of ordinary pin-joints as essential rotating parts of a lever.

Table 3. Characteristics of turntable

natural frequencies	p_{s3}	230 rad/s
	p_{s4}	210 rad/s
damping coefficients	ζ_{s3}	1.0
	ζ_{s4}	1.0
feedback loop gains	K_{P3}	102
	K_{D3}	0.883
	K_{P4}	108
	K_{D4}	1.03
sensitivity for disturbance	G_3	- 40 dB
	G_4	- 41 dB

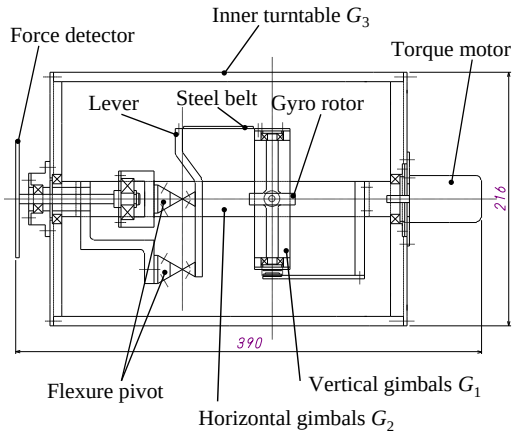

Figure 2. Construction model of GFMS

4. Characteristics of Response

4.1. Responses of GFMS

Now we consider responses of the GFMS with numerical simulations using these values and the following requirements:

・Force applied : F=0.3 [N]

(Initial load : F_0=0.3 [N])

・Angles of incidence : $\alpha = -45$, $\beta = -60$ [deg]

・Angles for step-changes in reference inputs:

$\Delta\eta_r$, $\Delta\varphi_r$ = 20 [deg]

・Time interval for step-changes of $\Delta\eta_r$ and $\Delta\varphi_r$:

Δt = 2 [s]

Figure 3 and 4 show responses of the measured outputs $\hat{F}$, η and φ in the GFMS.

It is confirmed that three outputs approach respective input values within about 10 [s]. The effect of nutation appears as transient, but it quickly damps out.

The error ε_F , which is in the steady-state of $\hat{F}$, is also shown in Figure 5. It is obvious that ε_F after 10 [s] represents sustained oscillation, which indicates the measured errors caused by small vibrations of the turntables due to the reaction torque of the GFMS [5].

4.2. Error Analysis

(1) Definition of Errors

We will now some systematic errors caused by various influences introduced in the GFMS.

Errors of the magnitudes of the force F and the angles of incidence are defined by

$$\left.\begin{aligned} \varepsilon_F &= \hat{F} - F \\ \varepsilon_\alpha &= \hat{\alpha} - \alpha \\ \varepsilon_\beta &= \hat{\beta} - \beta \end{aligned}\right\} \qquad (12)$$

where $\hat{F}$, $\hat{\alpha}$ and $\hat{\beta}$ are the outputs to the inputs F, α and β, respectively.

(2) ε_α and ε_β

From Equations 2 and 3, we get the following equations:

$$\left.\begin{aligned} \varepsilon_\alpha &= \frac{Fa\cos\varphi}{K_{P4}}\cos\psi + \frac{k_d\dot{\psi}}{K_{P4}}\sin\varphi - (\eta_r + \alpha) \\ \varepsilon_\beta &= -\frac{Fa}{K_{P3}}\sin\psi - (\varphi_r + \beta) \end{aligned}\right\} \qquad (13)$$

The first terms of ε_α and ε_β involve the oscillation component and the second terms of them do the dc-components. It should be noted that the dc-components are due to the estimation errors, namely tracking errors in servomechanisms. On the other hand, the amplitudes of the oscillation components are proportional to F and inversely prortional to K_{P3} and K_{P4} .

(3) ε_F

For the special case when $\varepsilon_\alpha = \varepsilon_\beta = 0$, the output $\hat{F}$ is given by

$$\hat{F} = -\frac{\omega}{a} H_0 \,. \qquad (14)$$

$$\left.\begin{aligned} \cos(\alpha+\eta) &= \cos\varepsilon_\alpha = 1 - \frac{1}{2}\varepsilon_\alpha^2 \\ \cos(\beta+\varphi) &= \cos\varepsilon_\beta = 1 - \frac{1}{2}\varepsilon_\beta \end{aligned}\right\}, \qquad (18)$$

we can finally get the following equation:

$$\varepsilon_F = -\frac{Fa}{2}(\varepsilon_\alpha^2 \cos\beta \cos\varphi + \varepsilon_\beta^2) \,. \qquad (19)$$

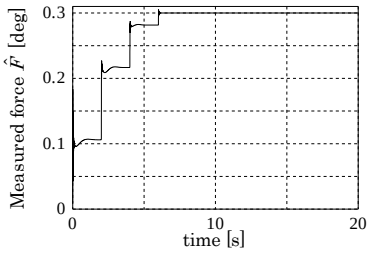

Fig. 4 Response of measured force $\hat{F}$

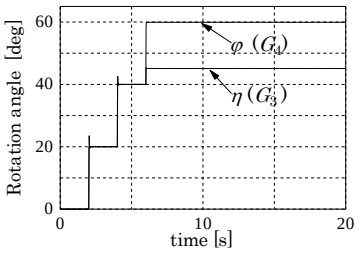

Fig. 5 Response of rotation angle of turntables

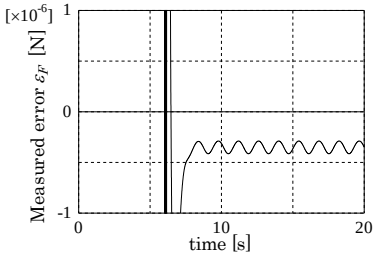

Fig. 6 Response of measured error ε_F

From this it follows that the GFMS will now maintain its virtually perfect linearity of precession rate ω against *F*. To find steady-state value ω we put $\ddot{\theta} = \dot{\theta} = \theta = 0$ and get

$$\omega = \frac{T_{1x1}}{H_0} \qquad (15)$$

Substituting Equation 2 and 15 into 14,we get the following equation in steady state

$$\hat{F} = F\{\cos\beta\cos\varphi\cos(\alpha+\eta) - \sin\beta\sin\varphi\} \qquad (16)$$

Thus, the error ε_F can be obtained from Equation.12

$$\varepsilon_F = F[\{\cos\beta\cos\varphi\cos(\alpha+\eta) - \sin\varphi\} - 1] \qquad (17)$$

Here, using the small approximations for ε_α and ε_β by

It is obvious that ε_F is strongly affected by the estimation errors ε_α and ε_β [6].

4.3. Relevance between k_d and θ

Finally, we will examine that there exists the upper and lower bounds on the derivative gain k_d in Equation 3. In the derivation process of errors, it is assumed that the deflection $\theta = 0$ in steady state. However, θ will not be vanished for a while just after *F* excites on the GFMS. Since the measured error increases as θ increases, it is crucial to settle θ to zero within the prescribed time interval for step-changes of $\Delta\eta_r$ and $\Delta\varphi_r$. The k_d has been introduced for the damping of nutation mode ζ_2, as shown in Figure 6. Taking the Laplace transform of the first and

Equation 2-1 and 2-2, the transfer function between the deflection $\Theta(s)$ and the input $F(s)a$ can be obtained by

$$\Theta(s) = -\frac{Bs^2 + c_2 + k_d s}{\Delta(s)} F(s)a \qquad (20)$$

where

$$\Delta(s) = (As^2 + c_1 s)(Bs^2 + c_2 s + k_d s) + H_0(H_0 s^2 + k_p s + k_i) \quad (21)$$

which denotes the characteristic equation of the gyroscope itself. From Equation 20, it fol- lows that θ is directly proportional to k_d. Choice of the k_d is important for obtaining meaningful sensors. A sketch of responses of θ for various ζ_2 is given in Figure 6. The larger ζ_2 to vanish θ leads to unacceptable response.

The condition for stability follows from Equation 21 as

$$k_d H_0 > B k_p \quad , \qquad (22)$$

and $$H_0^2 > B H_0 \frac{k_p}{k_d} + A\frac{k_i}{k_p} \qquad (23)$$

From the point of stability, small values of the k_d cause instability. As shown in Figure 6, the smaller ζ_2 becomes, the shorter the settling time for zeroing θ can be achieved. For ζ_2 less than 0.05, the response shows oscillatory pattern due to nutation mode. Thus, it is emphasized that for the choice of the k_d we have an appropriate range between the upper and lower bounds.

4.4 Effect of *F* on Errors

Figure 7 and 8 show the effect of the input force F on errors ε_α, ε_β and ε_F. In these Figures, the symbols "| |" and "—" denote the amplitude and the dc-component of oscillatory errors. It can be seen that ε_F has been gradually increased as F gets larger. This fact verifies that ε_F can be heavily affected by ε_α, ε_β and F.

Figure 9 shows the estimation errors $\eta_r + \alpha$ and $\varphi_r + \beta$ in servomechanisms. These curves exhibit the exactly same patterns as $\overline{\varepsilon_\alpha}$ and $\overline{\varepsilon_\beta}$, as shown in Figure 7. It can be concluded that ε_α and ε_β can be mainly determined by the estimation errors. To enable us to appreciate very high accuracies of the GFMS, the estimation errors should be reduced as small as possible.

Figure 10 shows the tracking errors of turntables for the reference inputs η_r and φ_r. The maximum error is little excess of 10^{-7} [deg]. For practical application, we can see that these errors do not influence the total amount of the estimation errors (less than 10^{-2} [deg]). It is also concluded that ε_α and ε_β are heavily varied with the estimation errors. There errors indicate theoretical limits of the accuracy of the GFMS.

6.Conclusions

A new gyroscopic force measuring system (simply called GFMS) was investigated as a vectorial force sensor to measure the magnitude and the direction of the force applied externally.The control structures and the estimator play important roles in determining the performance of the GFMS. In order to illustrate the effectiveness, some numerical analysis and simulations were conducted. The characteristics of both transient responses and errors were discussed and the limitations of the GMFS was clarified. At present, the GFMS has been in the works, and the practical applicability and the performance of it will be explored in industrial environment.

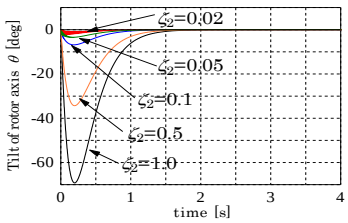

Fig. 7 Tilt of rotor axis θ in initial load due to damping coefficient ζ_2

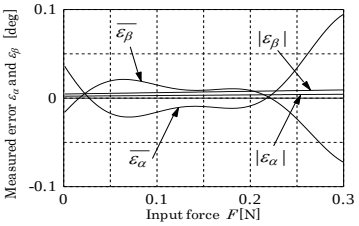

Fig. 8 Responses of measured error ε_α and ε_β due to input force F

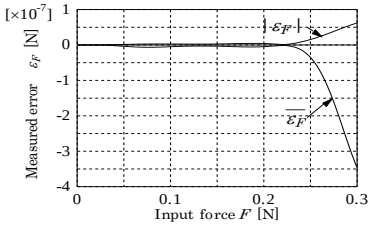

Fig. 9 Responses of measured error ε_F due to input force F

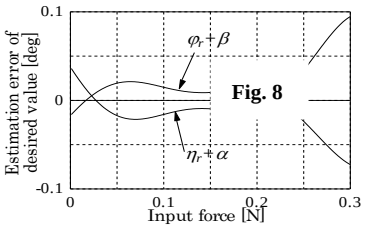

Fig. 10 Estimation errors of desired value due to input force F

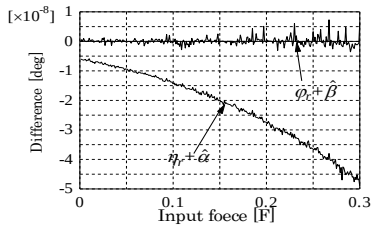

Fig. 11 Differences between desired values and rotation angles

7. References

[1]. Kurosu S., Kurosu M. Adachi, and Kamimura K., *Dynamical characteristics of gyroscopic weight measuring device,* ASME journal of Dynamic System, Measurement and Control, 1997, Vol.119, pp.346-350

[2] . Waagenbau W., Wöhl J., GmbH & Co., Postfach 7, D-7114 Pfedelbach.

[3]. Stevens C., & Son Ltd. "*Stevens-Wöhwa gyroscopic force measuring system*". 1979.

[4]. Kasahara M., Kurosu, Adachi S. M., and Kamimura K., "*Analysis of gyroscopic sensor applied to force measurement –vectorical measurement of horizontal force–*", IMEKO TC3/APMF'98, pp. 128-136, 1998

[5]. Kurosu S., Kasahara M., and Kodama K., *Gyroscopic Force Measuring System*, Proceedings of IMEKO XVI World Congress (Vienna, Austria), pp. 151-155 (2000)

[6]. Kasahara M., Kurosu S., Adachi M., and Kamimura K., *Analysis of a Gyroscopic Force Measuring System in Three-Dimensional Space*, Measurement **28**, pp.235-247 (2000)

Contact Person for Paper:

Dr. Shigeru Kurosu

Address : Oyama National College of Technology

771 Nakakuki, Oyama-city, 323-0806 Japan

Tel : 00-81-285-20-2201

Fax: 00-81-285-20-2880

E-mail: kurosu@oyama-ct.at.ac.jp